Structural Arrangement and Conformational Dynamics of the γ Subunit of the Na^+/K^+-ATPase†

Robert E. Dempski,‡ Janna Lustig,‡ Thomas Friedrich,|| and Ernst Bamberg*,‡,§

Department of Biophysical Chemistry, Max Planck Institute of Biophysics, Max-von-Laue-Strasse 3, D-60438 Frankfurt am Main, Chemical and Pharmaceutical Sciences Department, Johann Wolfgang Goethe University Frankfurt, Max-von-Laue Strasse 1, 7-9, D-60439 Frankfurt am Main, and Max-Volmer-Laboratory for Biophysical Chemistry, Institute of Chemistry, Secr. PC 14, Technical University of Berlin, Strasse des 17. Juni 135, D-60438 Berlin, Germany

Received September 3, 2007; Revised Manuscript Received October 8, 2007

ABSTRACT: The Na^+/K^+-ATPase couples the chemical energy in ATP to transport Na^+ and K^+ across the plasma membrane against a concentration gradient. The ion pump is composed of two mandatory subunits: the α subunit, which is the major catalytic subunit, and the β subunit, which is required for proper trafficking of the complex to the plasma membrane. In some tissues, the ion pump also contains an optional third subunit, γ, which modulates the pump activity. To examine the conformational dynamics of the γ subunit during ion transport and its position in relation to the α and the β subunits, we have used fluorescence resonance energy transfer under voltage clamp conditions. From these experiments, evidence is provided that the γ subunit is located adjacent to the M2−M6−M9 pocket of the α subunit at the transmembrane−extracellular interface. We have also used fluorescence resonance energy transfer to investigate the relative movement of the three subunits as the ion pump shuttles between the two main conformational states, E_1 and E_2, as described by the Albers−Post scheme. The results from this study suggest that there is no relative change in distance between the α and γ subunits but there is a relative change in distance between the β and γ subunits during the E_2 to E_1 transition. It was also observed that labeling the γ subunit at specific residues with fluorophores induces a decrease in K^+-induced stationary current. This result could be due to a perturbation in the K^+ branch of the reaction cycle of the pump, representing a new way to inhibit the pump.

The unequal distribution of Na^+ and K^+ ions across the plasma membrane in most animal cells is maintained by the Na^+/K^+-ATPase. This ion pump, which is a member of the P-type ATPase family as it is transiently phosphorylated at a highly conserved aspartate residue upon ATP hydrolysis, is comprised of two mandatory subunits. The large catalytic α subunit has approximately 1000 amino acids and 10 transmembrane domains and contains the binding sites for Na^+ and K^+ as well as for the specific cardiac glycoside inhibitors digitoxin and ouabain (*1*, *2*). The functional complex also includes a β subunit which is required for trafficking to the plasma membrane and modulates cation binding affinity (*3*−*5*).

In selected tissues, the Na^+/K^+-ATPase also can contain an optional third subunit, γ, which modulates the activity of the ion pump (*6*). The γ subunit is one of the FXYD family of proteins, which are found associated with the Na^+/K^+-ATPase in a tissue-specific manner (*7*). The γ subunit, or FXYD2, is predominantly expressed in the kidney together with the $\alpha_1\beta_1$-isozyme and was the first member of this family which was found to produce a functional effect on the Na^+/K^+-ATPase (*8*−*10*). It has been proposed that these effects, most notably a decreased affinity for intracellular Na^+, are of physiological relevance, as different segments of the renal nephron have distinct roles for the Na^+/K^+-ATPase in the Na^+ reabsorption process (*7*).

A significant advance in understanding the structure of all P-type ATPases was the elucidation of a series of conformations of the sarcoplasmic reticulum Ca^{2+}-ATPase (SERCA) by X-ray-crystallography (*11*, *12*). However, as the SERCA pump is comprised of only the catalytic α subunit, no information is available about the conformational flexibility of the β or γ subunits of the Na^+/K^+-ATPase. Thus, we have previously utilized voltage clamp fluorometry to measure the conformational dynamics of the Na^+/K^+-ATPase during ion transport. This was achieved by cysteine-specific labeling of the ion pump with the fluorescent dye tetramethylrhodamine-6-maleimide (TMRM).[1] We have shown that fluorescence changes that are induced by changes in membrane potential and/or ion concentrations (Na^+ and/or K^+) can be correlated to the two main conformational states,

† This work was supported by the Deutsche Forschungsgemeinschaft (Grant SFB 472), the Max Planck-Gesellschaft zur Förderung der Wissenschaften, and the Johann Wolfgang Goethe-Universität, Frankfurt am Main. R.E.D. was the recipient of a Max-Planck fellowship.

* To whom correspondence should be addressed. Fax: +49-69-6303-2222. Phone: +49-69-6303-2000. E-mail: ernst.bamberg@mpibp-frankfurt.mpg.de.

‡ Max Planck Institute of Biophysics.

§ Johann Wolfgang Goethe University Frankfurt.

|| Technical University of Berlin.

[1] Abbreviations: FRET, fluorescence resonance energy transfer; TMRM, tetramethylrhodamine-6-maleimide; FM, fluorescein-5-maleimide.

10.1021/bi701799b CCC: $40.75
Published on Web 12/15/2007

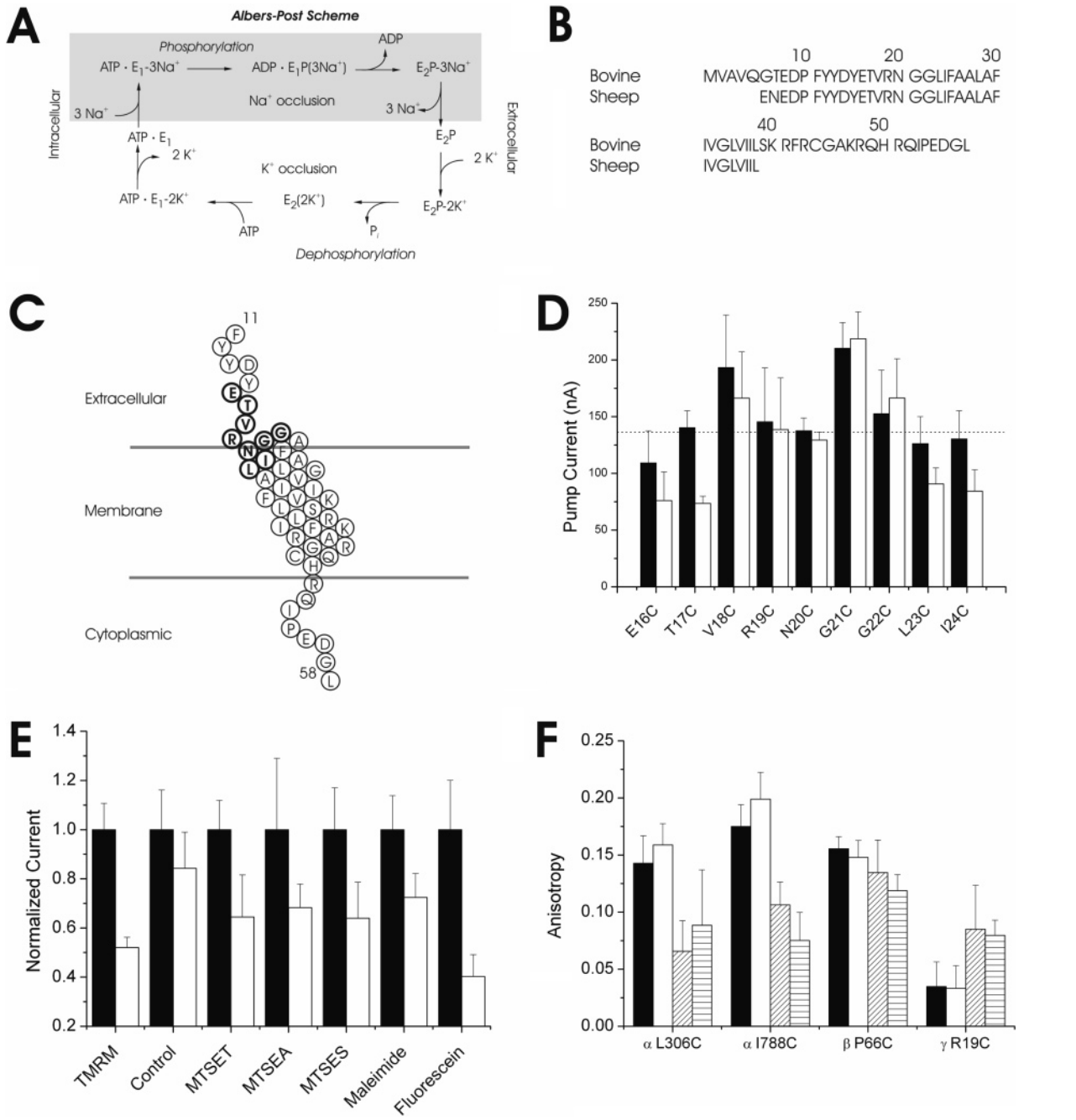

FIGURE 1: Reaction model and sequence and functional measurements of the Na^+/K^+-ATPase. (A) Albers−Post scheme for the Na^+/K^+-ATPase reaction cycle. (B) Sequence alignment of the bovine and sheep γ subunit. (C) Schematic diagram of the transmembrane domain and adjacent residues of the bovine γ subunit of the Na^+/K^+-ATPase. The diagram depicts residues Phe-11 to Leu-58; in bold are shown the nine residues Glu-16 to Ile-24, which were individually replaced by cysteines for the purpose of site-directed fluorescence labeling. (D) Stationary pump currents of the Na^+/K^+-ATPase are expressed with single-cysteine mutants of the γ subunit at a 0 mV holding potential in response to 10 mM K^+, before (black bars) and after (open bars) labeling with TMRM. Data originated from 5−8 oocytes; values are means ± SEM. The dotted line indicates the stationary current level of the wild-type construct. (E) Normalized stationary pump current for the $\alpha/\beta/\gamma$T17C construct before (black bars) and after (open bars) a 10 min incubation with select cysteine reactive labeling groups, including tetramethylrhodamine-6-maleimide (TMRM), [2-(trimethylammonium)ethyl]methanethiosulfonate (MTSET), (2-aminoethyl)methanethiosulfonate (MTSEA), (2-sufonatoethyl)methanethiosulfonate (MTSES), maleimide, and fluorescein-5-maleimide (fluorescein, FM). (F) Steady-state TMRM and FM anisotropy values for different residues of the ion pump in the presence of external Na^+ or K^+. Coding is as follows: black bars, TMRM in the presence of external Na^+; open bars, TMRM in the presence of external K^+; diagonally striped bars, FM in the presence of external Na^+; horizontally striped bars, FM in the presence of external K^+. All values are given as means ± SEM. Oocytes were clamped to −20 mV to maintain continuity between anisotropy and donor photodestruction measurements. Data originated from 5−8 oocytes.

E_1 and E_2, of the Na^+/K^+-ATPase as described by the Albers−Post scheme (Figure 1A) (*13*, *14*). Furthermore, we have been able to establish distance constraints between the α and β subunits of the Na^+/K^+-ATPase using fluorescence resonance energy transfer (FRET) after site-specific labeling of the α and β subunits with both donor and acceptor fluorophores and have been able to determine that there is a rearrangement between selected residues of the α and β subunits during the conformational transition of the ion pump (*15*).

Given the importance of the γ subunit in modulating the ion pump in select tissues, the aim of this study was to use voltage clamp fluorometry to investigate the interaction of the γ subunit with the holoenzyme. First, we have been able to establish distance constraints to model the location of the γ subunit when compared to the α and β subunits of the Na^+/K^+-ATPase proximal to the extracellular side of the plasma membrane of the ion pump. Second, we have been able to determine the relative movement of all three subunits as a function of ion transport. Third, it has been determined that labeling a specific residue on the γ subunit with the fluorophore TMRM or fluorescein-5-maleimide (FM) inhibits the ion pump. This inhibition appears to be mediated by steric effects, as charged cysteine-reactive moieties have little effect on the stationary current of the ion pump. The implication of these results, including the possibility of extending these results for γ-mediated, tissue-specific inhibition of the Na^+/K^+-ATPase, will be addressed.

EXPERIMENTAL PROCEDURES

Molecular Biology, Oocyte Preparation, and cRNA Injection. cRNA was obtained as previously described (*13*, *14*). Briefly, cDNAs of sheep Na^+/K^+-ATPase α_1 subunit with no extracellular cysteine residues (with mutations C911S and C964A) (*16*) and reduced ouabain sensitivity (with mutations Q111R and N122D) (*17*) for the selective inhibition of the endogenous Na^+/K^+-ATPase as well as the sheep β_1 subunit were subcloned into vector pTLN (*13*, *14*). The cattle γ subunit cDNA was synthesized (Sloning BioTechnology, Puchheim, Germany), sequenced, and also subcloned into vector pTLN. Single-cysteine mutations in the transmembrane−extracellular interface of the bovine γ subunit were introduced by the QuikChange site-directed mutagenesis kit (Stratagene) and verified by sequencing. cRNA was prepared using the SP6 mMessage mMachine kit (Ambion, Austin, TX).

Oocytes were obtained by collagenase treatment after partial ovarectomy from *Xenopus laevis* females and were injected with 25 ng of α subunit, 1 ng of β subunit, and 1 ng of γ subunit cRNA. After injection, the oocytes were kept in ORI buffer (90 mM NaCl, 2 mM KCl, 2 mM $CaCl_2$, and 5 mM MOPS, pH 7.4) containing 1 mg/mL gentamycin at 18 °C for 3−6 days before the measurements.

Oocyte Pretreatment and Fluorescence Labeling. Prior to the measurements, the oocytes were incubated for 45 min in loading buffer (110 mM NaCl, 2.5 mM sodium citrate, and 10 mM MOPS/Tris, pH 7.4) and 15 min in postloading buffer (100 mM NaCl, 1 mM $CaCl_2$, 5 mM $BaCl_2$, 5 mM $NiCl_2$, and 10 mM MOPS/Tris, pH 7.4) to elevate the intracellular Na^+ concentration (*18*). For stationary current measurements, cysteine-specific labeling was achieved by incubating the oocytes in Na^+ test solution containing FM or TMRM (Molecular Probes, Carlsbad, CA), (2-sulfonatoethyl)methanethiosulfonate (MTSES), [2-(trimethylammonium)ethyl]methanethiosulfonate (MTSET), or (2-aminoethyl)-methanethiosulfonate (MTSEA) (Gentaur, Brussels, Belgium), or maleimide (Sigma, St. Louis, MO) for 10 min in the measuring chamber. Stationary current measurements were obtained before and after cysteine-specific labeling following extensive washes in reagent-free buffer.

For donor (FM) photodestruction experiments, the method was performed as previously described (*15*). Briefly, the oocytes were incubated in either 5 μM FM or 1 μM FM and 4 μM TMRM for 30 min on ice in the dark followed by washes in dye-free buffer. At a 4:1 acceptor to donor fluorophore ratio, it is predicted that the ion pumps will be labeled pairwise at the following proportions: 4% FM/FM (D/D), 32% FM/TMRM (D/A), and 64% TMRM/TMRM (A/A). Thus, the predominant measured species will be the FM/TMRM pair, as the TMRM/TMRM pair will be excluded through the usage of the FRET filter set. Donor photodestruction measurements were performed in Na^+ test solution (100 mM NaCl, 5 mM $BaCl_2$, 5 mM $NiCl_2$, 10 μM ouabain, and 10 mM MOPS/Tris, pH 7.4) with continuous solution flow at −20 mV.

Two-Electrode Voltage Clamp Epifluorescence Measurements. An oocyte perfusion chamber was mounted on the stage of a fluorescence microscope (Axioskop 2FS, Carl Zeiss, Jena, Germany), equipped with a 40× water immersion objective (numerical aperture 0.8). Currents were measured using a two-electrode voltage clamp amplifier, Turbo TEC-05X (NPI Electronic, Tamm, Germany). Fluorescence was excited by a 100 W tungsten lamp. The following optical filter components were used: TMRM (535DF50 excitation filter, 565 EFLP emission filter, and 570DRLP dichroic mirror), FM (475DF40 excitation filter, 530DF30 emission filter, and 505DRLP dichroic mirror), and FRET (485AF20 excitation filter, 565 EFLP emission filter, and 505DRLP dichroic mirror) (Omega Optical, Brattleboro, VT). Fluorescence was measured with a PIN-022A photodiode (United Detector Technologies, Baltimore, MD) mounted to the microscope camera port. Photodiode signals were amplified by a patch clamp amplifier, EPC-5 (HEKA Electronics, Lambrecht, Germany). Fluorescence and current signals were simultaneously recorded and subsequently analyzed with Clampex 8.0 (Molecular Devices, Sunnyvale, CA) and Origin 7.5 (OriginLab Corp., Northampton, MA), respectively.

FRET and Anisotropy Measurements. For FRET distance measurements, irreversible donor photobleaching traces were usually fit to a monoexponential function. In some cases, the traces were best fit by a biexponential function where the time constant corresponding to the fast component was used and the slow time constant was only a small fraction of the total decay (*15*, *19*). The origin of the smaller slow component is unknown; however, it could be due to a diffusion process on the plasma membrane of the oocyte. To determine the efficiency of energy transfer (E), the following equation was used: $E = 1 - \tau_{DA}/\tau_D$ (where τ_{DA} and τ_D are the time constants of donor photobleaching in the presence and the absence of acceptor, respectively) (*20*). FRET efficiency was converted to distance using the Förster equation: $E = 1/(1 + R^6/R_o^6)$, where R is the distance between the donor and acceptor and R_o is the distance corresponding to 50% efficiency for a specific donor−acceptor pair (*20*). R_o is defined by the equation $R_o = ((9.7 \times 10^3)J\Phi_D n^{-4}\kappa^2)^{1/6}$ (Å), where J is the normalized spectral overlap of the donor emission and acceptor absorption, Φ_D is the donor emission quantum yield in the absence of the acceptor, n is the index of refraction, and κ^2 is the orientation factor for a dipole−dipole interaction (*21*).

Uncertainties in anisotropy and subsequent κ^2 calculations can lead to errors in the estimate of R_o since residues which exhibit significant polarized emission can limit the amount

of energy transfer between the donor and acceptor fluorophores and influence the distance measurements which are derived from irreversible fluorophore bleaching measurements (*22*). Therefore, the anisotropy of the donor and acceptor fluorophores was measured on the oocytes which represent a quasiplanar system and evaluated through the use of the following equation: $r = (I_{||} - I)/(I_{||} + 2I)$, where $I_{||}$ is the parallel and I is the perpendicular emitted light with respect to the polarized excitation light at each amino acid (Figure 1F) (*22*, *23*). The two components were measured sequentially with polarized filters (Linos Photonics, Inc., Göttingen, Germany) placed adjacent to the emission and excitation filters. To calculate the error in the distance measurements due to anisotropy, the following equations were used: $\kappa^2_{max} = {}^2/_3(1 + F_{rd} + F_{ra} + 3F_{rd}F_{ra})$ and $\kappa^2_{min} = {}^2/_3(1 - (F_{rd} + F_{ra})/2)$, where $F_{rd} = (r_d/r_o)^{0.5}$, $F_{ra} = (r_a/r_o)^{0.5}$, and r_o is the fundamental anisotropy (FM, 0.4; TMRM, 0.38) (*24*, *25*). For the αL306C/β/γR19C double mutant, the range of possible κ^2 values is 0.3−1.9. For the αI788C/β/γR19C double mutant, the range of possible κ^2 values was determined to be 0.3−2.0. For the α/βP66C/γR19C double mutant, the range of possible κ^2 values was determined to be 0.3−2.0. As the anisotropy measurements indicated that all of the residues had a reasonable mobility, κ^2 was assumed to be 2/3. Therefore, R_o was estimated for the FM/TMRM pair to be 55 Å.

Relative Movement of Specific Residues on the α, β, and γ Subunits. Determination of the relative movement of specific residues of different subunits during the E_2 to E_1 transition was performed as previously described (*15*). Double-cysteine mutant constructs were expressed where one residue is known to bind a fluorophore (i.e., demonstrates fluorescence changes during solution exchange that induce the E_2 to E_1 transition) and where it is unknown whether the second residue binds a fluorophore (i.e., no fluorescence changes during solution exchange). The double-cysteine mutant constructs were subsequently labeled with donor (FM) and acceptor (TMRM) fluorophores. A FRET filter set was used to excite the donor fluorophore and measure the emission of the acceptor fluorophore. Only when both sites have a bound fluorophore will one be able to observe a fluorescence change of TMRM which is the product of an environmental change of the fluorophore at the residue which demonstrates changes in fluorescence intensity during solution exchange that induce the E_2 to E_1 transition following energy transfer from the donor fluorophore. Using this strategy, the αN790C/β/γR19C construct was expressed. It was previously determined that the αN790C construct demonstrates a fluorescence change during the E_2 to E_1 transition (*14*). In contrast, although functional, no change in fluorescence intensity was observed for the γR19C construct if expressed with the α/β wild-type construct during the E_2 to E_1 transition following labeling with TMRM.

Following fluorophore labeling with FM and TMRM, the double-cysteine mutant construct exhibited a significant change in acceptor fluorescence intensity following donor excitation upon addition of 10 mM KCl, and the change in fluorescence intensity disappeared upon the addition of 10 mM ouabain, indicating that the change in fluorescence intensity is directly attributable to the Na^+/K^+-ATPase (data not shown). Thus, the γR19C construct is accessible to fluorophore labeling but is insensitive to the E_2 to E_1 transition. As three residues which are reactive with fluorophore labeling, but are insensitive to the E_2 to E_1 transition on either the α or the β subunits, have previously been identified (αL306C, αI788C, and βP66C), changes in the relative orientation of each of the three subunits were determined with the following double-cysteine constructs: αL306C/β/γR19C, αI788C/β/γR19C, and α/βP66C/γR19C (*15*).

Measurements and Analysis of Transient Currents. Transient Na^+/K^+-ATPase currents under Na^+/Na^+ exchange conditions were obtained as the difference between current responses to a specific voltage step in Na^+ test solution containing first 10 μM and second 10 mM ouabain to block the endogenous and heterologously expressed ouabain-insensitive forms of the Na^+/K^+-ATPase, respectively (*17*). Time constants were obtained from monoexponential fits to the data. The first few milliseconds after the voltage step were excluded to avoid artifacts arising from capacitance charging of the oocyte membrane. The displaced charge (Q) is the time intensity of the fitted currents, extrapolated to onset of the voltage pulses. The resulting $Q-V$ curves were fitted according to a Boltzmann function:

$$Q(V) = Q_{min} + \frac{Q_{max} - Q_{min}}{1 + e^{(z_q F(V_{0.5} - V)/RT)}}$$

where Q_{max} and Q_{min} are the saturation values of displaced charge, $V_{0.5}$ is the voltage of half-maximal activation, z_q is the fraction of charge that is displaced through the entire transmembrane field, F is the Faraday constant, R is the molar gas constant, T is temperature (K), and V is the transmembrane potential. All experiments were performed at 20−22 °C.

RESULTS

Site-Specific Labeling of the γ Subunit of the Na^+/K^+-ATPase. Our initial objective for this study was to examine the conformational dynamics of the γ subunit as a function of ion transport. Since our previous studies were carried out on sheep Na^+/K^+-ATPase, we attempted to obtain the sheep γ subunit sequence. Unfortunately, although sequencing efforts have begun on the sheep genome, the entire sequence of the γ subunit was not available. The only available sequence is a fragment which does not contain the entire coding sequence (*8*, *26*). However, as there are only two mutations between the sheep γ subunit fragment and the bovine sequence, both of which occur at the N-terminus of the protein, the bovine γ sequence was used for the experiments described in this paper (Figure 1B) (*8*, *26*).

Cysteine-scanning mutagenesis was performed to identify residues on the γ subunit at the cytoplasmic−transmembrane interface which demonstrate changes in fluorescence intensity as a function of membrane potential and/or external solution exchange (Figure 1C). Functional expression of each construct was assessed by measuring stationary pump currents upon addition of 10 mM K^+ in two-electrode voltage clamp experiments (Figure 1D). All solutions contained 10 μM ouabain to inhibit the endogenous Na^+/K^+-ATPase. It should be noted that all the constructs had a reduced ouabain sensitivity in the millimolar range, as shown for the sheep Na^+/K^+-ATPase α subunit (*17*). In coexpression experiments

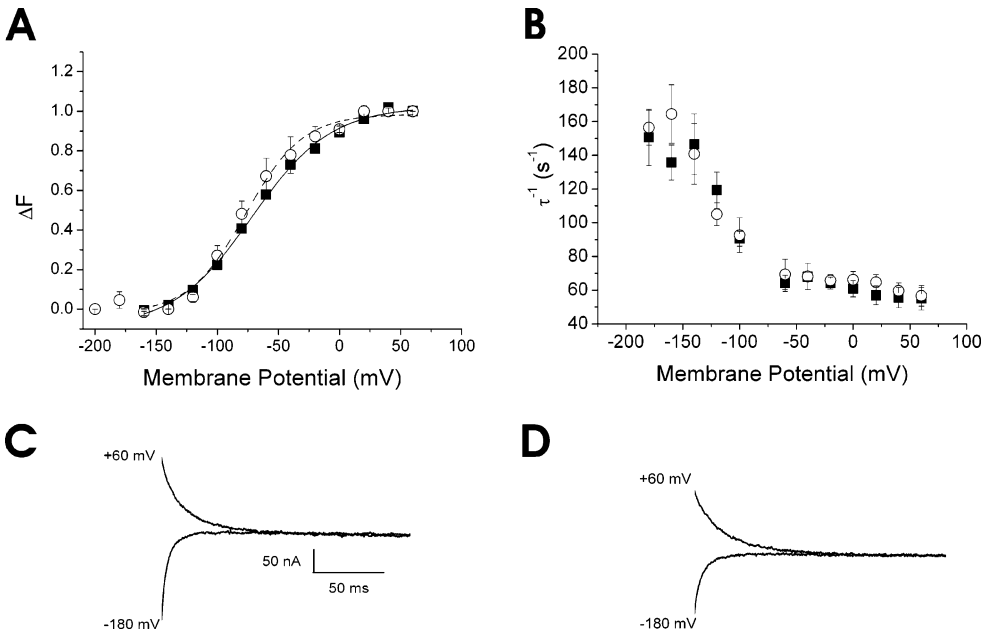

FIGURE 2: Voltage pulse-induced transient current measurements. (A) Voltage dependence of translocated charge for the $\alpha/\beta/\gamma$T17C construct of the Na^+/K^+-ATPase before (black squares) and after (open circles) labeling with fluorescein-5-maleimide. Data are means ± SEM from five oocytes. Fits of the Boltzmann function yielded the following parameters: before FM labeling, $V_{0.5} = -71 \pm 2$ mV, $z_q = 0.78 \pm 0.05$ (solid line); after FM labeling, $V_{0.5} = -77 \pm 3$ mV, $z_q = 1.1 \pm 0.1$ (dashed line). (B) Rate constants (reciprocal of time constants) for transient currents before (black squares) and after (open circles) FM labeling. Data are means ± SEM from five oocytes. (C) Voltage jump-induced transient currents, obtained as ouabain-sensitive difference currents recorded for the $\alpha/\beta/\gamma$T17C construct. (D) Voltage jump-induced transient currents, obtained as ouabain-sensitive difference currents recorded for the $\alpha/\beta/\gamma$T17C construct following labeling with FM.

with α and β subunits all nine cysteine mutants of the γ subunit led to functional ion pumps; however, no changes in fluorescence intensity for any of the TMRM-labeled mutants following a voltage jump or application of extracellular K^+ were observed. In contrast, it was observed that the stationary pump current was significantly reduced for three residues, T17C, L23C, and I24C, upon TMRM labeling. The most significant decrease in stationary current was observed upon fluorophore labeling of the $\alpha/\beta/\gamma$T17C construct.

To further investigate this observation, cysteine-specific labeling of the $\alpha/\beta/\gamma$T17C construct with a variety of moieties was achieved by incubating the oocytes in Na^+ test solution containing 5 μM labeling reagent for 10 min, followed by extensive washes in reagent-free buffer. The stationary current was measured before and after labeling. To examine whether charged groups would affect the function of the ion pump, the construct was labeled with three charged cysteine-reactive groups, MTSEA, MTSES, and MTSET (Figure 1E). MTSES is a negatively charged compound, while MTSEA and MTSET are positively charged, and each of these molecules has been used to probe the electrostatic interactions of a variety of membrane proteins such as the nicotinic acetylcholine receptor (*27*). Labeling the $\alpha/\beta/\gamma$T17C construct with these probes resulted in a small decrease in the stationary current; however, there was no significant difference in the decrease of the stationary current between the positively and negatively charged moieties.

As reported in the previous section, labeling the $\alpha/\beta/\gamma$T17C construct with TMRM had a dramatic effect on the stationary current, so we were interested to learn whether this was due to tetramethylrhodamine or maleimide. Thus, we labeled this construct with maleimide and observed that the stationary current was only modestly affected. To further determine whether the inhibition was specific to tetramethylrhodamine, we also labeled the ion pump with FM. It should be noted that FM, unlike fluorescein 5-isothiocyanate, which also inhibits the ion pump, reacts specifically with free cysteine residues, and no inhibitory effect of FM or TMRM was observed on the wild-type protein (*28*). Following stationary current measurements with and without FM, we observed the largest inhibition, where 38% of the original current was maintained. These data suggest that the inhibition of the ion pump that is mediated through labeling of the γ subunit is not due to charge, but is primarily due to the volume of the labeling reagents (see Figure 1E).

Transient Current Measurements. As it is clear that FM has the most dramatic effect upon the stationary current of the Na^+/K^+-ATPase, we were interested in further understanding the fluorophore-induced inhibition of the ion pump. Thus, we performed voltage pulses in the absence of K^+. Under these conditions, the Na^+/K^+-ATPase is restricted to Na^+/Na^+ exchange (*29*). Because dephosphorylation in the absence of K^+ is slow, the enzyme shuttles in a voltage-dependent manner almost exclusively between E_1P and E_2P. Information about the charge translocation process caused by the E_1P-E_2P conformational transition can be derived from analysis of the translocated charge. When plotted against the membrane potential, the amount of charge moved during a transient current follows a Boltzmann function (Figure 2A,C,D). Positive voltage pulses lead to maximal accumulation of E_2P, while negative pulses lead to accumulation of E_1P. As the charge movement occurs during the E_1P to E_2P conformational change, the $Q-V$ curve allows a direct measure of the amounts of E_1P and E_2P at any voltage. When compared to the α/β construct, the $V_{0.5}$ for the α/β/T17Cγ construct is not significantly different from

the wild-type value (−74 ± 12 mV vs −71 ± 2 mV for α/β vs α/β/γT17C, respectively). Following FM labeling of the α/β/γT17C construct, the $V_{0.5}$ for the Boltzmann distribution is shifted to a slightly more hyperpolarizing potential (−71 ± 2 mV vs −77 ± 3 mV for the unlabeled vs labeled α/β/γT17C construct, respectively), thus stabilizing the ion pump in the E_2P conformation. In addition, z_q, the fraction of charge that is displaced through the entire membrane field, is significantly increased following fluorescein-5-maleimide labeling of the α/β/γT17C construct (0.78 ± 0.05 vs 1.1 ± 0.1 for the unlabeled and labeled constructs, respectively).

We were further interested in measuring the transient current kinetics upon addition of FM. In these experiments, voltage jumps determine the kinetics of electrogenic reactions and shift the distribution between E_1P and E_2P, giving rise to transient currents. The main electrogenic events are the sodium binding steps, which occur on a microsecond time scale, but the detected transient charge movement is rate-limited by the conformational change $E_1P(Na) \leftrightarrow E_2P$ (Na) (*30*). Relaxation into a new distribution of states occurs with the sum of forward and backward reaction rate constants, and transient currents decay with first-order kinetics (*29*, *31*, *32*). Current signals were analyzed by fitting with a monoexponential function to obtain the voltage dependence of the apparent rate constants (Figure 2B−D). The transient currents of the α/β/γT17C construct at depolarizing membrane potentials drive the pump into the E_1P conformation, which enables electrogenic Na^+ reuptake, resulting in a negative transient current. The transient currents decayed at ∼60 s^{-1} at 0 mV, which agrees well with published data from *Xenopus* oocytes (*18*). At hyperpolarizing membrane potentials (−160 mV), the transient currents decayed at ∼160 s^{-1}, which is slower than that observed for previously published constructs which contained only the α and β subunits (*13*). The addition of FM, however, does not appear to have an appreciable effect on the transient current kinetics (Figure 2B).

As neither the charge distribution nor the transient current kinetics are dramatically altered upon labeling the α/β/γT17C construct with fluorescein-5-maleimide under Na^+/Na^+ exchange conditions and as there is a decrease in the amount of K^+-induced stationary pump current after FM labeling, the inhibition of the Na^+/K^+-ATPase by fluorophore labeling is most likely mediated through the K^+ branch of the Albers−Post scheme (Figure 1A).

Distance Measurements of the Ion Pump Subunits. To determine distance constraints between the γ subunit and the α or β subunit of the ion pump, the time dependence of donor photodestruction was measured following labeling with the donor fluorophore (FM) in the presence or absence of the acceptor fluorophore (TMRM) on double-cysteine constructs of the Na^+/K^+-ATPase as described previously (*15*). In these experiments, the observed photodestruction rate of the donor fluorophore depends on the donor cumulative excited lifetime (*15*). On a single-molecule level, the donor, when not paired to an acceptor fluorophore, has a long excited-state lifetime and, therefore, on a macroscopic level, photobleaches at a relatively fast rate (*33*). The excited-state lifetime of the donor fluorophore is shortened in the presence of an acceptor fluorophore due to energy transfer, which allows the donor, on a single-molecule level, to undergo more excitation cycles before photodestruction, which subsequently yields a slower macroscopic photobleaching. Furthermore, donor−acceptor pairs that are close together demonstrate a slower photodestruction rate of the donor fluorophore in the presence of the acceptor fluorophore when compared with a set of fluorophore-labeled residues that are further apart (*19*, *22*). Therefore, the difference between the rate of irreversible photodestruction of the donor fluorophore in the presence and absence of the acceptor fluorophore can be used to calculate the distance between the two fluorophores using the Förster equation (*20*).

For these experiments, the ion pump was labeled with either the donor alone or the donor and the acceptor fluorophores in a 1:4 ratio. At this ratio, if both the donor and acceptor fluorophores label the ion pump at the same rate at each residue (the chemistry is identical), the fluorophore ratio of double-cysteine constructs DD:DA:AA, where D is the donor fluorophore and A is the acceptor fluorophore, would be 0.04:0.32:0.64. The main component A/A is not observed due to the appropriate choice of the excitation and emission filters used during donor photodestruction measurements. Thus, the majority of fluorophores measured during donor photodestruction would be the D/A pair.

The rate of decay of the donor fluorophore, in the presence or absence of an acceptor fluorophore, was measured at a controlled membrane potential (−20 mV) under Na^+/Na^+ exchange conditions (0 mM K^+) to maintain a constant distance between subunits for three double-cysteine mutants (αI788C/β/γ19C, α306C/β/γ19C, and α/βP66C/γ19C). Each oocyte was tested for K^+-induced stationary currents, and only oocytes with a stationary pump current of greater than 100 nA were used for analysis. Each data set was normalized, averaged, and fit to a mono- or biexponential function. Distance measurements were calculated through the Förster equation and were determined to be 50.0 ± 0.2 Å for αI788C/β/γR19C, 62.9 ± 0.3 Å for α306C/β/γR19C, and 57.0 ± 0.2 Å for α/βP66C/γR19C (Figure 3A−C). It should be noted that these distance measurements do not directly take into account errors due to the effects of anisotropy, as κ^2 is assumed to be 2/3, and thus the error associated with these distance measurements could be larger than calculated above.

Relative Movements of the α, β, and γ Subunits during Ion Transport. A number of single-cysteine constructs of the Na^+/K^+-ATPase which are labeled with a fluorophore have been previously identified because the fluorescence intensity changes during the E_1 to E_2 transition and the fluorescence change are inhibited by high concentrations of ouabain (*13*, *14*). However, the majority (∼80%) of single-cysteine constructs demonstrate no fluorescence changes during the E_1 to E_2 transition of the ion pump, and these constructs have not been further studied. The absence of fluorescence change for these constructs has two possible explanations; either the residue is not accessible to the extracellular solution and cannot be labeled, or the residue is labeled with a fluorophore and there is no environmental change during the E_1 to E_2 transition. Thus, we developed a method to identify residues that were labeled with a fluorophore but were insensitive to the E_1 to E_2 transition to follow changes in FRET intensity following fluorophore labeling of two of these residues.

To identify residues which can be labeled with a fluorophore but where the fluorescence intensity is insensitive to

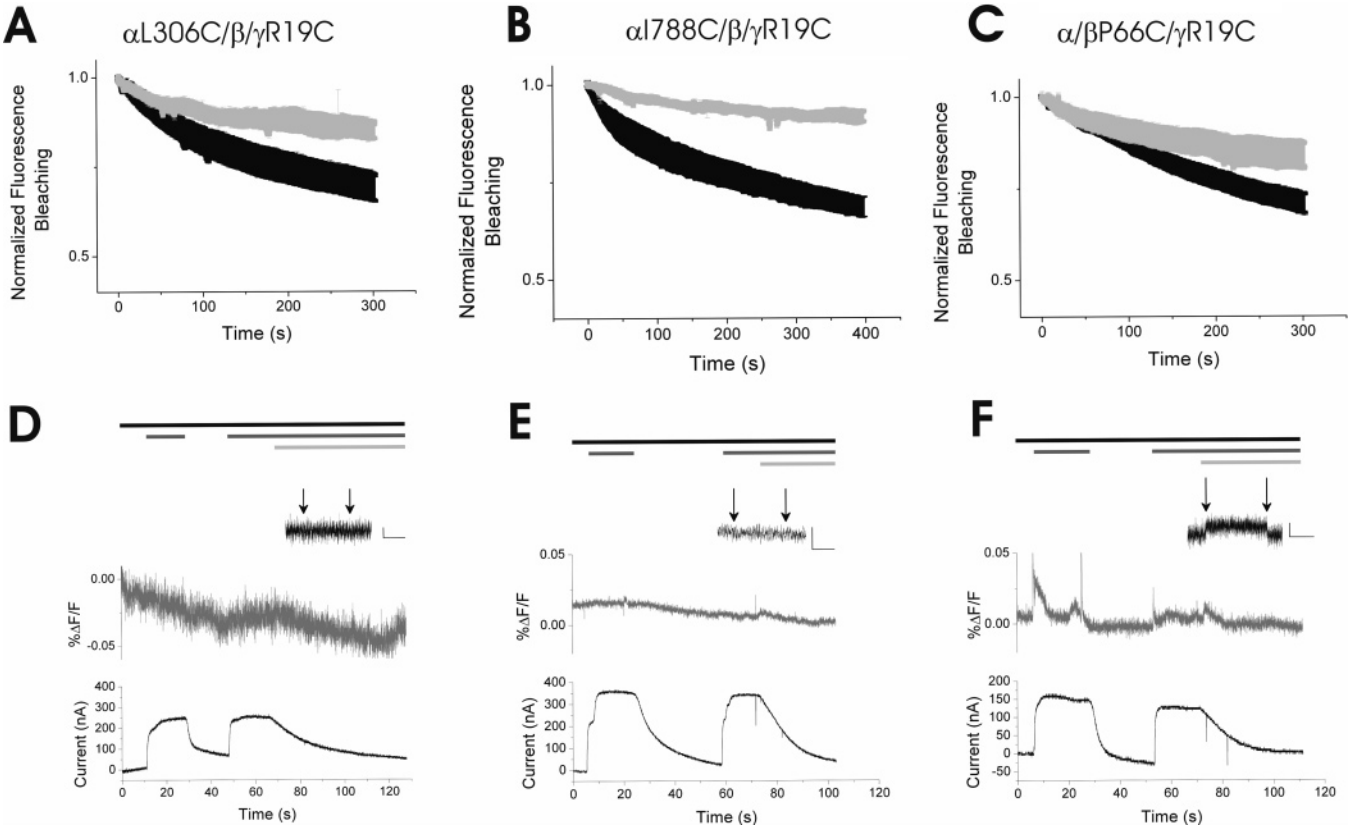

FIGURE 3: Distance measurements and relative movement of the α, β, and γ subunits of the Na^+/K^+-ATPase. (A−C) Normalized ΔF_{donor} photobleaching for the Na^+/K^+-ATPase αL306C/β/γR19C, αI788C/β/γR19C, and α/βP66C/γR19C constructs, respectively, labeled with donor fluorophore alone (black line) or donor plus acceptor fluorophore (gray line) in a 1:4 ratio. The results are the means of 4−7 oocytes ± standard error. The photodestruction rates for αL306C/β/γR19C are 99.7 ± 0.4 s^{-1} for the donor only and 144.3 ± 0.2 s^{-1} for the donor in the presence of acceptor. The photodestruction rates for αI788C/β/γR19C are 156.3 ± 0.9 s^{-1} for the donor only and 434 ± 2 s^{-1} for the donor in the presence of acceptor. The photodestruction rates for α/βP66C/γR19C are 161.1 ± 0.6 s^{-1} for the donor only and 291.0 ± 0.6 s^{-1} for the donor in the presence of acceptor. (D−F) Relative movement of the αL306C residue (M3−M4 loop) of the α subunit, the αI788C residue (M5−M6 loop) of the α subunit, and the βP66C residue (extracellular−transmembrane interface of the β subunit) in relation to the γR19C residue (extracellular−transmembrane interface of the γ subunit), respectively. Parallel recording of the pump current (lower, black) and fluorescence resonance energy transfer change (upper, gray) at −40 mV under Na^+/Na^+ exchange conditions (black bars) in response to 10 mM K^+ (dark gray bars) and 10 mM ouabain (light gray bars). Results are from a single oocyte, but the experiments were repeated, with essentially identical results, on at least four occasions. The inset of each figure (in black) shows the fluorescence response to a change in membrane potential from 0 to −200 mV (arrows indicate the onset and offset of the membrane potential pulse) where the scale bars on the *x* and *y* axes are 0.01% $\Delta F/F$ and 200 ms, respectively.

the E_1 to E_2 transition, double-cysteine mutant constructs were expressed where one residue is known to bind a fluorophore (i.e., demonstrates fluorescence changes during solution exchange) and where it is unknown whether the second residue binds a fluorophore (i.e., no fluorescence changes during solution exchange). The constructs were subsequently labeled with donor (FM) and acceptor (TMRM) fluorophores. In these experiments, we were not measuring the relative movement of the two cysteine residues. Instead, one cysteine is used as a relay to transfer energy to the second residue. Only when both sites have a bound fluorophore will one be able to observe a fluorescence change which is the product of the environmental change of TMRM at one residue. It is irrelevant which of the two residues has a donor or acceptor fluorophore as each pairing will exhibit the same result. If, on the other hand, only one of the two residues is labeled, no change in acceptor fluorescence intensity will be observed.

Residues on the M3−M4 (αL306C) and M5−M6 (αI788C) loops of the α subunit as well as at the transmembrane−extracellular interface of the β subunit (βP66C) have previously been identified which can be labeled with fluorophores but are insensitive to changes in membrane potential and/or solution exchange (*15*). Using the strategy outlined above, we identified a residue on the γ subunit, R19C, which could be labeled with a fluorophore but did not demonstrate fluorescence changes upon changes in membrane potential and/or external solution exchange (data not shown). Following this step, double-cysteine constructs were expressed to determine whether there was a conformational rearrangement of the γ subunit when compared to the α or β subunits of the Na^+/K^+-ATPase (*15*).

Neither the αL306C/β/γR19C construct nor the αI788C/β/γR19C construct demonstrated a change in fluorescence intensity of the acceptor fluorophore following donor excitation upon addition of 10 mM KCl (Figure 3D,E). In contrast, the α/βP66C/γR19C construct exhibited a significant change in fluorescence intensity of the acceptor fluorophore following donor excitation upon addition of 10 mM KCl (Figure 3F). This fluorescence change is directly attributable to the Na^+/K^+-ATPase as the FRET intensity change is abolished following the addition of 10 mM ouabain. One concern from these experiments was that unequal solution exchange would result in a fluorescence artifact where a change in fluores-

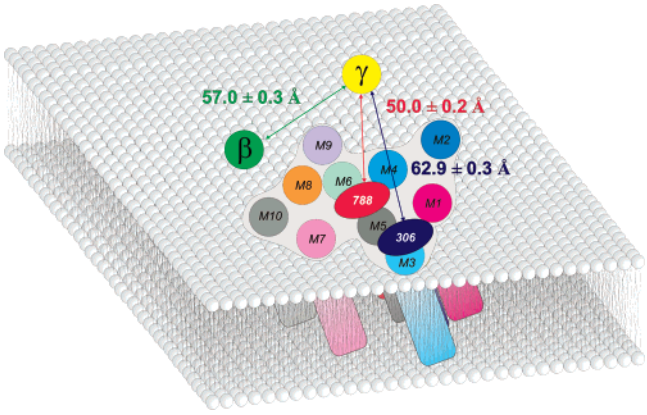

FIGURE 4: Two-dimensional helix arrangement viewed from the surface of the cell, including 10 transmembrane helices which form the α subunit (M1−M10), the transmembrane domains of the *β* (in green) and the *γ* (in yellow) subunits, and the distance constraints determined in this study. Distance constraints were determined using residues αL306C (in blue), αI788C (in red), *β*P66C, and *γ*R19C.

cence intensity would be observed. In fact, it was seen that a transient fluorescence signal is observed following addition and removal of external K^+ in Figure 3F. Therefore, changes in fluorescence intensity were measured following voltage pulses from 0 to −200 mV, which eliminates any artifact which might arise as a function of solution exchange (Figure 3D−F, inset). The change in FRET is also not due to a change in the orientation of the donor and/or acceptor fluorophore dipoles between the E_1 and E_2 conformations as there is no significant change in anisotropy for either FM or TMRM at any of the residues tested in either external Na^+ or external K^+ (Figure 1F).

DISCUSSION

The results from this study have resolved distance constraints between the *γ* subunit and the α or *β* subunit of the Na^+/K^+-ATPase. Our data agree qualitatively with electron microscopy studies, cross-linking experiments, and functional effects of mutations in TM9 (*34*−*36*). However, the distance constraints obtained from donor photodestruction measurements suggest that the *γ* subunit is not directly adjacent to the M2−M6−M9 groove of the α subunit, but is somewhat distal from the α subunit at the transmembrane−extracellular interface (Figure 4). It is important to note that the distance measurements have been interpreted in a two-dimensional model by assuming that the residues are located in the same plane parallel to the cell membrane. As both the M3−M4 and the M5−M6 loops on the α subunit are only six residues long and the residues from the *β* and *γ* subunits are proposed to be adjacent to the plasma membrane according to hydropathy analysis, this assumption is reasonable. If, however, the residues are located at different distances from the plasma membrane, then the FRET measurements will overestimate the intersubunit distances, and the residues will seem further apart in our model when compared with a true three-dimensional model. In addition, if *γ* subunits are present in the plasma membrane which are not associated with the holoenzyme, this would result in a population of subunits which could be labeled with fluorescein, without an associated acceptor fluorophore. This would result in a decay curve for the donor/acceptor pair which is faster than a decay curve of only the holoenzyme and would subsequently result in an overestimation of the distance between the *γ* subunit and either the α or *β* subunit. Thus, in this instance, the distance constraints determined in this paper would be the outer limit for the orientation of the *γ* subunit when compared to the holoenzyme. It has been determined that the *γ* subunit can be isolated as an oligomer in native kidney membranes (*37*). However, it is unknown whether these oligomers are present after the ion pump is expressed in *Xenopus* oocytes.

In contrast to static intermediate structures determined by crystallography, our studies can also be used to obtain insight into the relative movement of the three subunits during ion translocation. By identifying residues proximal to the plasma membrane−extracellular interface of all three subunits, where the fluorescence intensity is insensitive to the conformational dynamics of the holoenzyme, it is possible to study the relative movement of specific residues of the ion pump following labeling with donor and acceptor fluorophores. From these experiments, it was determined that no large conformational rearrangement is observed between residues on either the M3−M4 or the M5−M6 loop of the α subunit when compared to the *γ* subunit. This result is consistent with the observation that no residues on the *γ* subunit demonstrated a change in fluorescence intensity following changes in the external ionic conditions and/or membrane potential as the environment of the *γ* subunit is unchanged during ion transport. However, it was observed that there is a conformational rearrangement between the *β* and *γ* subunits proximal to the transmembrane−extracellular interface of the ion pump during the E_2 to E_1 transition. Thus, although the α and *γ* subunits move together during the E_2 to E_1 transition, there is a significant relative conformational rearrangement between the α and *γ* subunits when compared to the *β* subunit during ion translocation. It should be noted that it is unlikely that there is zero relative movement between the α and *γ* subunits during the E_2 to E_1 transition as it is well established the fifth transmembrane domain undergoes a conformational rearrangement during ion transport (*38*). Most likely, the relative movement between these subunits is below the limit of detection for the fluorescein−rhodamine FRET pair and is less than the relative movement of the *γ* subunits when compared to the *β* subunit during the conformational transition of the ion pump. It is likely that the *β* subunit undergoes the largest relative movement when compared to the α or *γ* subunit, especially considering that it has already been demonstrated that the *β* subunit has two distinct tryptic digest profiles when the holoenzyme is in the E_1 or E_2 conformation, which suggests that the *β* subunit undergoes a large conformational rearrangement during the E_2 to E_1 transition (*39*).

The results from our experiments have also determined that labeling selected residues of the *γ* subunit inhibits the ion pump. Further development of this observation could prove rewarding, as the Na^+/K^+-ATPase has been implicated in the pathogenesis of many diseases, including bladder, renal, and prostrate cancers (*40*). However, as the ion pump is ubiquitously expressed in all cell types, utilization of a broad inhibitor of the Na^+/K^+-ATPase would have only a limited benefit. As the *γ* subunit is primarily expressed in the kidney, identification of drugs which could selectively bind to the wild-type *γ* subunit and inhibit the ion pump could have an important therapeutic benefit in selective

anticancer drugs, such as the treatment of kidney/urinary tract cancers, where it has already been identified that a high concentration of digitoxin lowers the risk for this cancer (*41*).

At this point, inhibition of the ion pump, induced by cysteine-specific labeling of the γ subunit, is not well understood. It has previously been determined that the γ subunit induces an increase in V_{max} and $K_{0.5}$ for Na^+ as well as a decrease in the $K_{0.5}$ for K^+ at hyperpolarizing membrane potential when expressed in *Xenopus* oocytes (*42*). However, following fluorophore labeling of the $\alpha/\beta/\gamma$T17C construct, the reduced stationary current is not accompanied by a dramatic shift in transient current kinetics nor in $V_{0.5}$, although it appears that the inhibition is mediated by steric effects and that the addition of either TMRM or FM affects the K^+ branch of the Albers−Post scheme. Whether this inhibition is specific to the γ subunit or can be expanded to other members of the FXYD families of proteins is also an unresolved question.

Previously, site-directed mutagenesis and protein modeling as well as electron microscopy studies have suggested that the FXYD proteins are docked within the M2−M4−M9 cavity of the α subunit (*34*, *36*). In addition, tryptophan-scanning mutagenesis has been employed to examine the interaction between FXYD7 and the α subunit of the Na^+/K^+-ATPase (*43*). From these studies, it was proposed that there are two faces of the FXYD7 protein, one where the amino acids are implicated in the structural and/or functional association of the ion pump and therefore face the α subunit of the ion pump and one where there is no structural and/or functional association of the Na^+/K^+-ATPase and where these residues face away from the ion pump. Following homology modeling of the γ subunit and the FXYD7 protein, the γT17C residue is predicted to be located at the interface of these two regions and oriented toward the M2 transmembrane domain. Thus, it is plausible that inhibition of the Na^+/K^+-ATPase could be uniquely mediated at this position as the residue is both accessible to fluorophore labeling and adjacent to the α subunit of the ion pump.

Thus, from our measurements we have been able to resolve distance constraints between the three subunits of the Na^+/K^+-ATPase by selectively labeling double-cysteine constructs. We have been able to determine that there is no conformational rearrangement between the α and γ subunits, but there is a rearrangement between the β and γ subunits proximal to the transmembrane−extracellular interface of the ion pump during the E_1 to E_2 transition. These data complement an earlier finding, where it was determined that there is a conformational rearrangement between the α and β subunits proximal to the transmembrane−extracellular interface of the ion pump during the E_2 to E_1 transition (*15*). Finally, we have identified a novel way to inhibit the ion pump, by selectively labeling a residue on the γ subunit of the Na^+/K^+-ATPase, which underlines the tight coupling of the γ subunit to the function of the pump.

REFERENCES

1. Jørgensen, P., and Pedersen, P. (2001) Structure-function relationships of Na^+, K^+, ATP, or Mg^{2+} binding and energy transduction in Na,K-ATPase, *Biochim. Biophys. Acta 1505*, 57−74.
2. Kaplan, J. H. (2002) Biochemistry of the Na,K-ATPase, *Annu. Rev. Biochem. 71*, 511−535.
3. Geering, K., Theulaz, I., Verrey, F., Hauptle, M. T., and Rossier, B. C. (1989) A role for the beta-subunit expression of functional Na^+K^+-ATPase in the *Xenopus* oocyte, *Am. J. Physiol. 257*.
4. Beguin, P., Hasler, U., Beggah, A., Horisberger, J., and Geering, K. (1998) Membrane integration of Na,K-ATPase alpha subunits and beta subunits assembly, *J. Biol. Chem. 273*, 24921−24931.
5. Geering, K., Beggah, A., Good, P., Girardet, S., Roy, S., Schaer, D., and Jaunin, P. (1996) Oligomerization and maturation of Na,K-ATPase: Functional interaction of the cytoplasmic NH_2 terminus of the beta subunit with the alpha subunit, *J. Cell Biol. 133*, 1193−1204.
6. Bibert, S., Roy, S., Schaer, D., Felley-Bosco, E., and Geering, K. (2006) Structural and functional properties of two human FXYD3 (Mat-8) isoforms, *J. Biol. Chem. 281*, 39142−39151.
7. Geering, K. (2005) Function of FXYD proteins, regulators of Na,K-ATPase, *J. Bioenerg. Biomembr. 37*, 387−392.
8. Mercer, R. W., Biemesderfer, D., Bliss, D. P., Collins, J. H., and Forbush, B. (1993) Molecular cloning and immunological characterization of the gamma-polypeptide, a small protein associated with the Na+/K+-ATPase, *J. Cell Biol. 121*, 265−266.
9. Therien, A. G., Goldshleger, R., Karlish, S. J., and Blostein, R. (1997) Tissue-specific distribution and modulatory role of the gamma subunit of the Na+/K+-ATPase, *J. Biol. Chem. 272*, 32628−32634.
10. Luecking, K., Nielsen, J. M., Pedersen, P. A., and Jorgensen, P. L. (1996) Na-K-ATPase isoform abundance in rat kidney estimated by competitive RT-PCR and ouabain binding, *Am. J. Physiol. 271*, F253−260.
11. Toyoshima, C., Nakasaki, M., Nomura, H., and Ogawa, H. (2000) Crystal structure of the calcium pump of sarcoplasmic reticulum at 2.6 angstrom resolution, *Nature 405*, 647−655.
12. Toyoshima, C., and Nomura, H. (2002) Structural changes in the calcium pump accompanying the dissociation of calcium, Nature Structural changes in the calcium pump accompanying the dissociation of calcium, *Nature 418*, 605−611.
13. Dempski, R. E., Friedrich, T., and Bamberg, E. (2005) The beta subunit of the Na+/K+-ATPase follows the conformational state of the holoenzyme, *J. Gen. Physiol. 125*, 505−520.
14. Geibel, S., Kaplan, J. H., Bamberg, E., and Friedrich, T. (2003) Conformational dynamics of the Na^+/K^+-ATPase probed by voltage clamp fluorometry, *Proc. Natl. Acad. Sci. U.S.A. 100*, 964−969.
15. Dempski, R. E., Hartung, K., Friedrich, T., and Bamberg, E. (2006) Fluorometric measurements of intermolecular distances between the alpha and beta subunits of the Na+/K+-ATPase, *J. Biol. Chem. 281*, 36338−36346.
16. Hu, Y. K., and Kaplan, J. H. (2000) Site-directed chemical labeling of extracellular loops in a membrane protein-The topology of the Na,K-ATPase alpha-subunit, *J. Biol. Chem. 275*, 19185−19191.
17. Price, E. M., and Lingrel, J. B. (1988) Structure-function-relationships in the Na,K-ATPase alpha subunit: Site-directed mutagenesis of glutamine-111 and asparagine-122 to aspartic acid generates a ouabain-resistant enzyme, *Biochemistry 27*, 8400−8408.
18. Rakowski, R. F. (1993) Charge movement by the Na/K pump in *Xenopus oocytes*, *J. Gen. Physiol. 101*, 117−144.
19. Glauner, K. S., Mannuzu, L. M., Gandhi, C. S., and Isacoff, E. Y. (1999) Spectroscopic mapping of voltage sensor movement in the Shaker potassium channel, *Nature 402*, 813−817.
20. Forster, T. (1948) Intermolecular energy migration and fluorescence, *Ann. Phys. 2*, 55−75.
21. Van Der Meer, B. W., Coker, G., and Chen, S. Y. D. (1994) *Resonance Energy Transfer: Theory and Data*, Wiley, New York.
22. Lakowicz, J. (1999) *Principles of Fluorescence Spectroscopy*, 2nd ed., Kluwer Academic/Plenum Publishers, New York.
23. Dale, R., Eisinger, J., and Blumberg, W. (1979) The orientational freedom of molecular probes, *Biophys. J. 26*, 161−194.
24. Cha, A., and Bezanilla, F. (1998) Structural implications of fluorescence quenching in the Shaker K^+ channel, *J. Gen. Physiol. 112*, 391−408.
25. Chen, R., and Bowman, R. (1965) Fluorescence polarization: Measurement with ultraviolet-polarizing filters in spectrophotofluormeter, *Science 147*, 729−732.
26. Collins, J., and Leszyk, J. (1987) The "gamma subunit" of Na,K-ATPase: a small amphiphillic protein with a unique amino acid sequence, *Biochemistry 26*, 8665−8668.

27. Stauffer, D. A., and Karlin, A. (1994) Electrostatic potential of the acetylcholine binding sites in the nicotinic receptor probed by reactions of binding-site cysteine with charged methanethiosulfonates, *Biochemistry 33*, 6840−6849.
28. Karlish, S. J. (1980) Characterization of conformational changes in (Na,K) ATPase labeled with fluorescein at the active site, *J. Bioenerg. Biomembr. 12*, 111−136.
29. Nakao, M., and Gadsby, D. C. (1986) Voltage dependence of Na translocation by the Na/K pump, *Nature 323*, 628−630.
30. Holmgren, M., Wagg, J., Bezanilla, F., Rakowski, R. F., De Weer, P., and Gadsby, D. C. (2000) Three distinct and sequential steps in the release of sodium ions by the Na^+/K^+-ATPase, *Nature 403*, 898−901.
31. Friedrich, T., and Nagel, G. (1997) Comparison of Na^+/K^+-ATPase pump currents activated by ATP concentration or voltage jumps, *Biophys. J. 73*, 186−194.
32. Holmgren, M., and Rakowski, R. F. (1994) Pre-steady-state transient currents mediated by the Na/K pump in internally perfused *Xenopus* oocytes, *Biophys. J. 66*, 912−922.
33. Mannuzu, L. M., Moronne, M. M., and Isacoff, E. Y. (1996) Direct physical measure of conformational rearrangement underlying potassium channel gating, *Science 271*, 213−216.
34. Hebert, H., Purhonen, P., Vorum, H., Thomsen, K., and Maunsbach, A. (2001) Three-dimensional structure of renal Na,K-ATPase from cryo-electron microscopy of two-dimensional crystals, *J. Mol. Biol. 314*, 479−494.
35. Lindzen, M., Gottschalk, K., Füzesi, M., Garty, H., and Karlish, S. J. (2006) Structural interactions between FXYD proteins and Na,K-ATPase, *J. Biol. Chem. 281*, 5947−5955.
36. Li, C., Grosdidier, A., Crambert, G., Horisberger, J. D., Michielin, O., and Geering, K. (2004) Structural and functional interaction sites between Na,K-ATPase and FXYD proteins, *J. Biol. Chem. 279*, 38895−38902.
37. Mahmmoud, Y. A., Vorum, H., and Cornelieus, F. (2000) Identification of a phospholemman-like protein from shark rectal glands, *J. Biol. Chem. 275*, 35969−35977.
38. Lutsenko, S., Anderko, R., and Kaplan, J. H. (1995) *Proc. Natl. Acad. Sci. U.S.A. 92*, 7936−7940.
39. Lutsenko, S., and Kaplan, J. H. (1994) Molecular events in close proximity to the membrane associated with the binding of ligands to the Na,K-ATPase, *J. Biol. Chem. 269*, 4555−4564.
40. Chen, J., Contreras, R., Wang, R., Fernandez, S., Shoshani, L., Russo, I., Cereijido, M., and Russo, J. (2006) Sodium/potassium ATPase (Na+, K+-ATPase and ouabain/related cardiac glycosides: a new paradigm for development of anti-breast cancer drugs, *Breast Cancer Res. Treat. 96*, 1−15.
41. Beguin, P., Wang, X., Firsov, D., Puoti, A., Claeys, D., and al, e. (1997) The gamma subunit is a specific component of the Na,K-ATPase and modulates its transport function, *EMBO J. 16*, 4250−4260.
42. Garty, H., and Karlish, S. J. (2006) Role of FXYD proteins in ion transport, *Annu. Rev. Physiol. 68*, 431−459.
43. Li, C., Crambert, G., Thuillard, D., Roy, S., Schaer, D., and Geering, K. (2005) Role of the transmembrane domain of FXYD7 in structural and functional interactions with Na,K-ATPase, *J. Biol. Chem. 280*, 43738−42743.

BI701799B